# IDENTIFICATION OF BREAST VASCULAR CALCIUM DEPOSITION IN DIGITAL MAMMOGRAPHY BY LINEAR STRUCTURE ANALYSIS

*Jie-Zhi Cheng*[1], *Chung-Ming Chen*[1], *Dinggang Shen*[2*]
[1] Institute of Biomedical Engineering, National Taiwan University
[2] Dept. of Radiology and BRIC, University of North Carolina at Chapel Hill
[*]dinggang_shen@med.unc.edu

## ABSTRACT

Computerized detection of vascular calcium depositions in mamagraphy is a new research topics, which is driven by the clinical hypothesis of the association with many related cardiovascular diseases. In several previous studies [7, 9], calcification cue plays a very important role in the computerized analysis. We observe that vascular calcium depositions can be identified with high confidence if they appear in a bright railway pattern. Accordingly, a linear structure analysis method is introduced in this study to detect most true calcifications and also keep the false positives as little as possible. The proposed method is tested with 40 mammograms and achieves performance of 93.8±1.3% in sensitivity and 84.7±3.9% in specificity. The output of this linear structure analysis may provide more reliable calcification cue for the subsequent vessel tracking process, which will be investigated in the future.

***Index Terms***— Breast vascular calcification, Mammography, Linear structure analysis

## 1. INTRODUCTION

Breast arterial calcification (BAC) in digital mammography has recently been reevaluated as a potential biomarker that may associate with coronary heart disease [1], diabetes [2], hypertension [2, 3] and so on. Although the connection to the coronary heart disease remains controversial [4], other links to diseases, like chronic kidney disease [5], bone mineral density reduction [6], etc., are also continuously being investigated, with positive results. In many previous clinical studies [1-6], the identification of BAC was mostly conducted by hand. This manual process is often subjective and tedious. Especially when the data size goes formidably large, the manual identification may be far impractical. In this case, the computerized detection of BAC in digital mammography deems to be in a need to facilitate the clinical analysis and hypothesis validation.

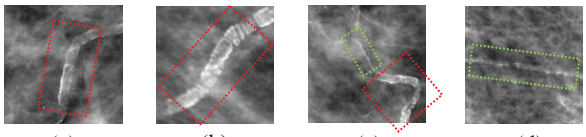
In the literature, there are quite few studies relevant to computerized detection of BAC in mammography, as the clinical topics and demand are relatively new. Ge *et al.* developed a detection method with calcification cue [7]. In their method, calcifications were first identified by globally thresholding on the image convolved with the calcification enhancement filter [8]. A principal curve clustering technique was then developed to find the regression curves from the point cloud of calcification candidates. In the final stage, a classifier was applied to reduce false positives. Cheng *et al.* [9] leveraged the calcification and vesselness cues in a random-walk tracking framework to reconstruct the complicated structure of vessels with calcium deposition. Seeded by the calcification cues, the random-walk tracking process rendered multiple sampling paths from the vesselness map to depict candidate tracts of calcified vessels in a mammogram. A latter compiling and linking process was thus performed to organize and link up the obtained sampling paths. This random-walk tracking framework was shown to be capable of addressing issues of vessel branching, overlapping, and disconnection due to the 2D mammographic projection.

Although some promising results were demonstrated in [9], the seeding strategy utilized in [9] may have chance to retrieve too many false sampling tracts, which could conceivably make the subsequent compiling and linking tasks more arduous. The calcification cue in [9] was computed in a similar way of [8]. Specifically, the calcification points are selected by a global threshold on the image convolved with calcification enhance filter [8]. Just like the common problem shared by many thresholding techniques, the global threshold which can be universally applied to any case is very difficult to determine. For instance, a conservative threshold may lead to many false calcification candidates, while an aggressive threshold could possibly exclude many important seeds. Motivated by this concern, a linear structure analysis method is developed in this paper to address the globally thresholding problem. The linear structure analysis is based on the result of [8] with a conservative global threshold. The main purpose of the proposed linear structure analysis method is to keep the true points of calcium deposition as many as possible while reduce significantly the false calcification seeds at the same time.

## 2. METHOD

Breast arterial calcification (BAC) is a phenomenon of calcium deposition along vascular lumen in breast. In a

mammogram, vessel with calcium deposition may appear like bright railways (parallel linear structures) under proper 2D projection view, as shown in Figure 1(a-b). Comparing to other appearance patterns (Figure 1(c-d)), this kind of bright railway pattern can be more certainly labeled as parts of calcified vessels with much less inter-observer disagreement. Accordingly, it may be particularly of help if we are able to locate the bright railways in a mammogram as the basis of further analysis.



(a) (b) (c) (d)

**Fig. 1.** Example patterns of breast vascular calcium depositions in digital mammography.

In this paper, we adopt a method in [8] to first collect calcification candidates with a conservative threshold. Then, a parallel linear structure detector is carried out to locate those calcification points which hold bright railway patterns. Because those points identified by the parallel linear structure detector can be parts of the vascular calcium deposition with high confidence, we are able to estimate the distribution of the true vascular calcium deposition in a feature space. With the knowledge of feature distribution, we can specifically define a range to reject those points beyond the estimated range.

Due to the effect of 2D projection, some calcification points may possibly constitute as a single linear structure, as those indicated by the green dotted rectangles in Figure 1(c-d). To find out this kind of calcium depositions and rule out more false calcifications, a single linear structure detector is applied as the final step to identify those survival points within the estimated range in the feature space. In the following, we will introduce every step of the linear structure analysis to achieve the identification of the true breast vascular calcium deposition with satisfactory performance.

**2.1. Calcification Detection with Conservative Threshold**

The basic idea of the calcification detection technique in [8] is constituted into two major steps. First, the calcification signals are enhanced by the difference between the two smoothed images from different image filter kernels. Similar to [8], the enhanced difference image was computed by subtracting a Gaussian-smoothed image from another smoothed image by a special filter with its kernel defined as: $f = [2f_A - 1]f_B$, where $f_A$ is a low-pass smoothing filter and $f_B$ is a high-frequency noise-suppressing filter. In this paper, $f_A$ is set as a Gaussian filter with standard deviation of 4.5 and $f_B$ is defined as a mean filter.

Then, a global thresholding technique is subsequently applied to collect at most $N$ highest response points in the filtered image, denoted as $F$, as the detected calcifications. More specifically, this can be achieved by finding the minimal intensity threshold $t$, such that the number of the thresholded points is no larger than $N$:

$$\{p_t\} = min_t\{p \mid \forall p \in F, F(p) \geq t\}, \text{s.t.} \|\{p\}\| \leq N, \quad (1)$$

where $\{p_t\}$ is the point set of the collected calcification candidates. $t$ is a threshold, and $N$ is set as 8000 in this study. More details of the calcification detection technique can be referred to [8].

**2.2. Parallel Linear Structure Detector**

We are interested in finding out the bright railway portions in a mammogram and take them as parts of vascular calcium deposition. In a 2D calcification map which is plotted by the obtained point set $\{p_t\}$, the bright railways appear as parallel linear structure patterns. The desired parallel linear structures may be oriented in various directions. Moreover, the parallel linear structures usually appear disconnected due to sporadic calcium deposition and are surrounded by other false-detected calcifications; see Figure 2 for examples. Hence, the detector for parallel linear structures should be invariant to the vessel orientations and also robust to sporadic calcium deposition. To this end, the parallel linear structures are detected by the two following steps: (1) local orientation estimation, and (2) projective profile analysis along the estimated local orientation. We obtain the projection profile by convolving the local window of the point of interest with several line integral functions. These line integral functions are oriented with the same estimated local direction, but are parameterized with different distance offsets from the center of the local window. For the efficiency of computation, the detection process is only applied to the geometric center of each connected component in the calcification map.

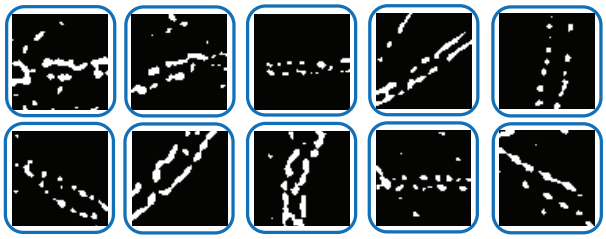


**Fig. 2.** Examples for several parallel linear structures.

Specifically, to obtain the projection profiles, the orientations of the local structures are estimated first. Given a circular local window, $W_p(x,y)$, of the calcification map which is centered at the centeroid $p$ of the current connected component, the local orientation $v_p$ can be estimated by:

$$v_p = arg_v \max \int_{-B_x}^{B_x} \int_{-B_y}^{B_y} W_p(x,y) D(L_v(x,y)) dxdy, \quad (2)$$

where $L_v(x,y)$ is an integral line function of the angle $v$ and is defined as $xcosv + ysinv$. The connected component is a subset of $\{p_t\}$ and hence the centroid $p$ also belongs to $\{p_t\}$. In equation (2), $D(\cdot)$ is Dirac's delta function, and $B_x$ and $B_y$ are the half of window sizes in $x$ and $y$ dimensions of the

local window $W_p(x,y)$, respectively. For robustness, the local orientation of the current connected component is averaged with other estimated local orientations in the neighboring connected components.

Similar to Radon transform, the projection profiles can be derived by integrating along the estimated local orientation with different distance offsets. Given the local window $W_p(x,y)$ centered at point $p$, the projection profile along the estimated orientation $v_p$, with respect to different distance offset γ, can be obtained as:

$$Prof_{v_p}(\gamma) = \int_{-B_x}^{B_x}\int_{-B_y}^{B_y} W_p(x,y) D\left(L_{\gamma,v_p}(x,y)\right) dxdy. \quad (3)$$

Where $L_{\gamma,v_p}(x,y)$ is the integral line along the angle $v_p$ with a distance offset $\gamma$. Again, $D(\cdot)$ is Dirac's delta function, and $B_x$ and $B_y$ are the half of window sizes in $x$ and $y$ dimensions of the local window $W_p(x,y)$, respectively.

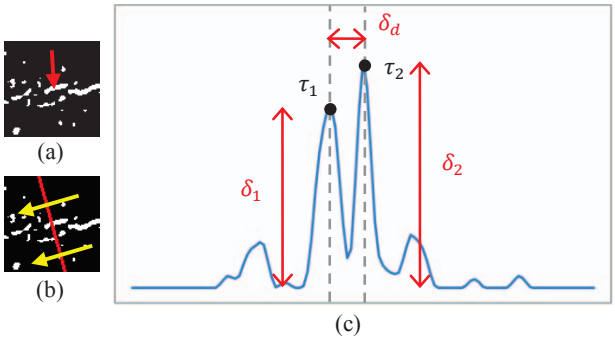



**Fig. 3.** Illustration of projection profile analysis of the calcification cluster indicated by the red arrow in (a). (a) ROI of a calcification map; (b) projection of spatial calcification distribution; (c) the obtained projection profile after smoothing.

The one dimensional projection profile $Prof_v(\gamma)$ of a parallel linear structure along the local orientation is expected to have dual strong peaks near to the center of the profile. Since the peak here is the local maximum in the projection profile, one dimensional watershed transformation is performed to obtain all local maxima in the profile. As the projection profile could be noisy, the profile is smoothed before applying watershed transformation. Then, we seek the two strongest peaks near to the center of profile such as $\tau_1$ and $\tau_2$ in Figure 3. If both peaks, $\tau_1$ and $\tau_2$, are stronger than a given threshold, $\delta_s$, and the distance between the two peaks is within a specific distance, denoted as $\delta_d$, the profile is considered having dual strong peaks. Since the local orientation $v_p$ is estimated, we can perform the mentioned dual strong peaks analysis on several other projection profiles, $Prof_v(\gamma)$, with a specific range of orientations around the estimated one, i.e., $\forall\, v \in \{v_p - 6^\circ,\ v_p - 3^\circ,\ v_p,\ v_p + 3^\circ,\ v_p + 6^\circ\}$. If one of the projection profiles possesses the dual strong peaks around the center, the current tested connected component will be regarded as a part of one parallel linear structure. In this study, the two thresholds, $\delta_s$ and $\delta_d$, are learnt from a set of manually-labeled samples of parallel linear structures and will be detailed in the experiment section. Figure 3 demonstrates the whole process of projection profile analysis for the parallel linear structures in calcification map.

### 2.3. Exclusion of False Calcium Deposition and Preserving of Single Linear Structure

The parallel linear structure detector selects a subset, $\{p_t^l\}$, from the point sets $\{p_t\}$ in the equation (1), as calcification candidates with bright railway patterns. The point subset $\{p_t^l\}$ can help us to exclude those points which are far different from the true calcifications. Recalling that the feature image, $F$, is the filtering result with the calcification enhancement filter, we are able to calculate the mean $\mu_t^l$ and standard deviation $\sigma_t^l$ of the parallel linear structures from the feature set $\{F(p_t^l)\}$. With these statistics, we can discard any point $p_t^d$ in $\{p_t\}$ which satisfies $F(p_t^d) < \mu_t^l - \alpha\sigma_t^l$. Here, $\alpha$ is a discarding factor which is set as 1.0 in our study. After the exclusion process, we have a set of the candidate points $\{p_t^e\} = \{p_t\}/\{p_t^d\}$.

Due to the 2D projection effect and sporadic deposition, some calcifications may appear like a single line, instead of railway. Hence, we intend to discover those points, denoted as $p_t^s$ which spatially constitute a single linear structure, from the result of the exclusion process $\{p_t^e\}$. This discovery process is similar to the task of finding parallel linear structures in $\{p_t\}$, but only one peak is considered. As the locations of the parallel linear structures have already been known, we can only find those single linear structures in the set $\{p_t^{e/l}\} = \{p_t^e\}/\{\{p_t^e\} \cap \{p_t^l\}\}$. We select the points in the set $\{p_t^{e/l}\}$ which hold a single peak strength larger than $\beta_s$ in the projection profile $Prof_{v_s}(\gamma)$, and denote the collected point set of single linear structures as $\{p_t^s\}$. Distinct from the parallel linear structure detector, the parameter $\beta_s$ is empirically set as 8 as it is less important in the whole process of linear structure analysis. We output the joint point set $\{p_t^s\} \cup \{\{p_t^e\} \cap \{p_t^l\}\}$ as the candidate set of vascular calcium depositions.

## 3. EXPERIMENTS AND RESULTS

The best parameter setting of the parallel linear structure detector is obtained via learning from the training samples. To find the best parameters of $\delta_s$ and $\delta_d$, we arbitrarily select 800 positive samples from a pool of the true parallel linear patterns collected from expert's annotations in 20 mammograms. Meanwhile 800 negative samples, which include background and single linear structure patterns, are also prepared for a balanced learning. We randomly divide the training data into 4 sets and perform 4-fold cross-validation to obtain a good parameter setting. In each fold of cross-validation, 600 positive and 600 negative samples are taken as training data. The remaining 400 samples are treated as testing data.

The best learnt parameter setting of $\delta_s$ and $\delta_d$ achieves the performance of sensitivity 92.0%, 94.5%, 93.0% and

92.5% for the testing data in each of 4 folds of cross-validation, respectively. The respective specificity rates are 85.5%, 83.0%, 84.5% and 87.5%.

We test our linear structure analysis method on 40 new digital mammograms. For the performance analysis, we compare the computerized results with the expert's identifications. As it is infeasible to manually pick the calcifications in a pixel-by-pixel fashion, we provide a user interface to allow user to draw a box to identify a group of true calcium deposition on the calcification map. Figure 4 show a demonstration result with the manual identification. Figure 4(b) is the result of calcification detection with conservative threshold, and Figure 4(c) depicts the parallel linear structures. The final result is shown in Figure 4(d) where we can see that the most desired calcium depositions are found and also the false calcification points are removed significantly. We can also preserve some vascular calcium depositions with single linear structure pattern (as indicated by yellow arrow) and some subtle depositions with parallel linear structure pattern (as indicated by green arrow). Figure 4(e) exhibits the manual identification. The overall detection performance on the 40 new mammograms reaches 93.8±1.3% for sensitivity and 84.7±3.9% for specificity.

## 5. CONCLUSION

A new computerized detection method for the vascular calcium deposition in mammography is introduced in this paper. Experimental results show that the major calcifications can be found by the proposed method, at the same time reducing many false calcification points. The detected calcium depositions can provide more reliable calcification cues for the subsequent process of extracting the whole calcified vessels in mammography. Specifically, the proposed method may potentially boost the performance of random-walk tracking scheme [9] by alleviating its complexity in the compiling and linking process.

## 4. REFERENCES


[1] M.A. Rotter, P.F. Schnatz, A.A. Jr. Currier and D.M. O'Sullivan, "Breast Arterial Calcification (BACs) Found on Screening Mammography and Their Association with Cardiovascular Disease," *Menopause*, 15: pp. 276-281, 2008.

[2] J.M. Kemmeren, D. Beijerinck, P.A. van Noord, J.D. Banga, J.J. Deurenberg, F.A. Pameijer and Y. van der Graaf, "Breast Arterial Calcifications: Association with Diabetes Mellitus and Cardiovascular Mortality - Work in Progress," *Radiology,* 201: pp. 75-78, 1996.

[3] M. Cetin, R. Cetin, N. Tamer and S. Kelekçi, "Breast Arterial Calcifications Associated with Diabetes and Hypertension," *Journal of Diabetes and Its Complications,* 18: pp. 363-366, 2004.

[4] M.H. Zgheib, *et al.*, "Breast Arterial Calcifications on Mammograms Do Not Predict Coronary Heart Disease at Coronary Angiography," *Radiology*, 254: pp. 367-373, 2010.

[5] V. Duhn, E.T. D'Orsi, S. Johnson, C.J. D'Orsi, A.L. Adams and W.C. O'Neill, "Breast Arterial Calcification: A Marker of Medial Vascular Calcification in Chronic Kidney Disease," *Clinical Journal of the American Society of Nephrology*, 6(2): pp. 377-382, 2011.

[6] J. Reddy, J.P. Bilezikian, S.J. Smith and L. Mosca, "Reduced Bone Mineral Density is Associated with Breast Arterial Calcification," *Journal of Clinical Endocrinology & Metabolism*, 93: pp. 208-211, 2008.

[7] J. Ge, *et al.*, "Automated Detection of Breast Vascular Calcification on Full-field Digital Mammograms," *Proc. SPIE* 6951, 695117, 2008.

[8] H.P. Chan, *et al.*, "Computer-aided Detection of Mammographic Microcalcifications: Pattern Recognition with an Artificial Neural Network," *Medical Physics*, 22: pp. 1555-1567, 1995.

[9] J.Z. Cheng, E.B. Cole, E.D. Pisano and D. Shen, "Detection of Arterial Calcification in Mammograms by Random Walks," *IPMI 2009*, LNCS, 5635: pp. 713-724, 2009.

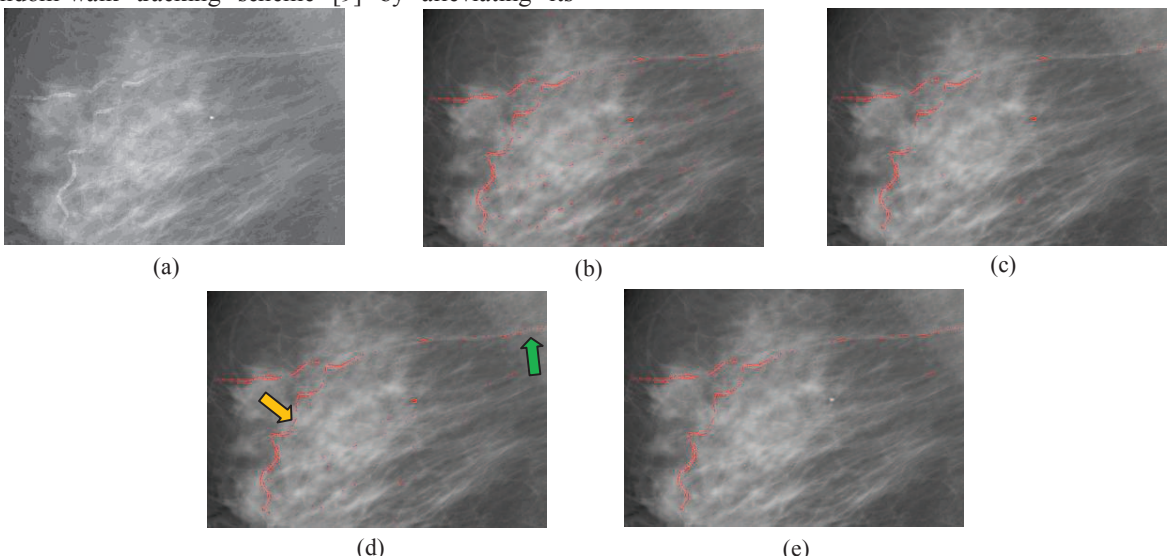




**Fig. 4.** Demonstration of detection result on one sample. (a) A mammogram; (b) calcifications found by the method [8]; (c) calcifications with parallel linear structure patterns; (d) final result; and (e) manual identification result.